Analytica Chimica Acta 1335 (2025) 343440

Contents lists available at ScienceDirect

Analytica Chimica Acta

journal homepage: www.elsevier.com/locate/aca

Multiplex digital PCR for the simultaneous quantification of a miRNA panel

Florence Busato [a], Sylvain Ursuegui [b], Jean-François Deleuze [a], Jorg Tost [a,*]

[a] Laboratory for Epigenetics & Environment, Centre National de Recherche en Génomique Humaine, CEA-Institut de Biologie François Jacob, Université Paris-Saclay, Evry, France
[b] Stilla Technologies, Biopark 1, Mail du Professeur Georges Mathé, 94800, Villejuif, France

HIGHLIGHTS

- MiRNA signatures represent promising biomarkers for clinical applications.
- First proof-of-concept of a multiplexed digital PCR assay for miRNA analysis.
- Combination of miRNA-specific stem-loop primers and dPCR with hydrolysis probes.
- Linear and reproducible quantification results for up to six miRNAs.
- Optimised protocol can be applied to different types of biological samples.

GRAPHICAL ABSTRACT

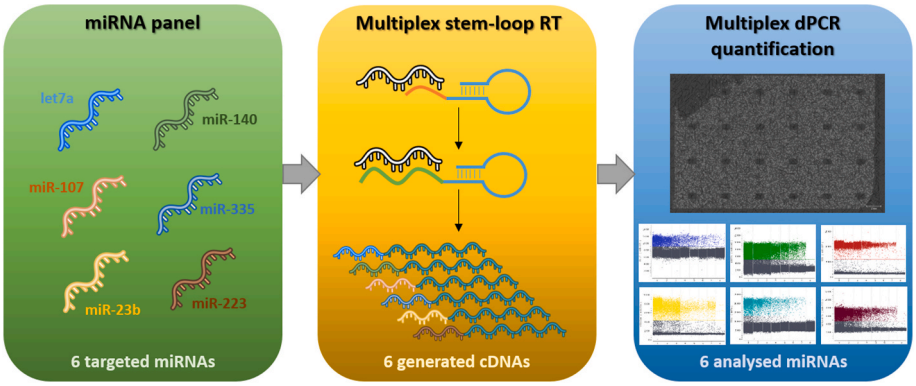

ARTICLE INFO

Handling Editor: J.P. Landers

Keywords:
Digital PCR
microRNA
Stem-loop primer
Personalised medicine
Multiplex analysis
microRNA signature

ABSTRACT

Background: microRNAs (miRNAs) are small non-coding RNAs regulating gene expression. They have attracted significant interest as biomarkers for early diagnosis, prediction and monitoring of treatment response in many diseases. As individual miRNAs often lack the required sensitivity and specificity, miRNA signatures are developed for clinical applications. Digital PCR (dPCR) is a sensitive fluorescent-based quantification method, that can be used to detect the expression of miRNAs in patient samples. Our study presents the first proof-of-concept of a multiplexed dPCR assay for the simultaneous analysis and quantification of multiple miRNAs.
Results: After reverse transcription (RT) using a pool of miRNA-specific stem-loop primers, dPCR was performed with a universal reverse primer and miRNA-specific forward primers along with fluorescently-labelled hydrolysis probes. Multiple experimental parameters were evaluated and strategies for modulating the observed signals were devised. The optimised assay was applied to the analysis of miRNAs from cell lines and biological samples. Although absolute quantification was lost, due to the reverse transcription step, quantification was linear for the dilution series and results were highly reproducible for independent dPCR and RT reactions. Our results confirmed the high sensitivity of dPCR for patient samples.
Conclusions: We demonstrate the feasibility and reliability of multiplexed detection and quantification of miRNAs by dPCR that can be applied in a clinical setting to evaluate miRNA signatures.

* Corresponding author. Laboratory for Epigenetics & Environment, Centre National de Recherche en Génomique Humaine, CEA-Institut de Biologie François Jacob, 2 rue Gaston Crémieux, Evry, France.
E-mail address: tost@cnrgh.fr (J. Tost).

https://doi.org/10.1016/j.aca.2024.343440
Received 28 August 2024; Received in revised form 7 November 2024; Accepted 18 November 2024
Available online 20 November 2024

1. Introduction

Digital PCR (dPCR) was developed in the 1990s to quantify nucleic acids using a fluorescent assay (hydrolysis probe or intercalating dye) similar to quantitative PCR (qPCR), but with improved sensitivity for some applications such as detection of mutations and viral/bacterial sequences [1]. dPCR is based on partitioning samples in a limiting dilution to obtain positive (1) or negative (0) partitions, hence the name of "digital" in analogy to the binary language of informatics. Partitioning can be obtained through the generation of water-oil emulsion droplets or by distributing the PCR mix into nanowell plates with a microfluidic system. dPCR has become a frequently used method for the detection and quantification of nucleic acids. dPCR-based assays have therefore been implemented in clinical practice, especially for applications in bacteriology, virology, non-invasive prenatal testing and oncology.

MicroRNAs (miRNAs) are a family of small non-coding RNAs between 21 and 24 nucleotides in size. The human genome codes for around 2600 miRNAs [2]. miRNAs modulate gene expression post-transcriptionally by promoting the degradation of mRNA transcripts or hindering their translation by binding to their 3′UTR. They contribute to all fundamental biological processes from development and differentiation to cell cycle regulation, constructing complex gene regulatory networks as most human genes are regulated by one or several miRNAs [3]. miRNAs are relatively stable nucleic acid-based biomolecules that can be reliably analysed from various biological sources including liquid biopsies independent of their storage conditions and are less impacted by sample degradation [4,5]. They have therefore attracted substantial interest as biomarkers for the early detection and classification of cancer and other human diseases as well as predicting and monitoring treatment response [6,7]. Single miRNAs do not often have the required sensitivity and/or specificity to be used as a reliable biomarker for these applications. Therefore, commonly signatures combining several miRNAs are used. To further improve the diagnostic value, miRNA expression signatures are combined for some applications with other clinical and molecular features. For instance, computed tomography in combination with a 24-miRNA signature for the detection of lung cancer significantly reduced false positive rates compared to tomography alone [8]. In epithelial ovarian cancer, the MIROvaR predictor signature consisting of 35 miRNAs can detect early relapse of patients with ovarian cancer [9]. Furthermore, a five-miRNA signature was devised differentiating patients with colorectal cancer or advanced adenoma from healthy individuals [10]. However, these signatures have not yet reached clinical routine implementation and are currently under validation in prospective studies and clinical trials (e.g. MIROvaR [11,12]; lung cancer CT [13,14]). Nonetheless some miRNA assays have already been commercialized as CE-marked in vitro diagnostic medical device including miR-31-3p for the prediction of anti-EGFR response in colorectal cancer (miRpredX 31-3p®, Integragen, France) [15], a three-miRNA signature for the assessment of the risk for hepatectomy post liver failure (hepatomiR®, TAmiRNA, Austria) [16] or 11 miRNAs used for risk stratification of thyroid cancer patients in the absence of strong driver mutations (ThyraMIR®v2, Interspace Diagnostics, US) [17].

qPCR assays, and especially locked nucleic acid (LNA)-enhanced qPCR assays, are currently considered to be the gold standard for miRNA expression analysis in clinical applications because of their wide dynamic range and low limit of detection [18]. dPCR constitutes an alternative analytical approach for miRNA analysis and has been found to improve reproducibility and accuracy compared to qPCR especially for biological material available only in limited quantities [19,20]. Both intercalating dye chemistry as well as hydrolysis probes can be used and showed similar performance with a high sensitivity down to one miRNA copy/µL [21]. However, the complexity of the biological samples as well as the multiple steps required for the isolation of the miRNAs will lead to a reduced sensitivity in practice. dPCR has been less frequently used for miRNA analysis compared to qPCR as it is less easily performed in standardized high-throughput settings. dPCR has for example been used for the analysis of miR-652-3p as a biomarker for the multi tyrosine kinase inhibitor Regorafenib [22] as well as for deciphering and quantifying let-7b-5p in a regulatory network associated with favourable prognostics in oestrogen receptor positive breast cancer [23]. dPCR miRNA analysis has been applied to determine the tissue of origin for cancers of unknown origin using an 89-miRNA panel [24]. However, these analyses were commonly performed using intercalating dyes for target detection and thus targeting a single miRNA per reaction requiring multiple reactions for the analysis of miRNA signatures. Hydrolysis probes labelled with two different fluorophores have been used to detect two miRNAs, mostly the target and a reference miRNA, in a duplex format using dPCR [25].

Recently, several dPCR instruments were commercialized that allow the simultaneous multicolour detection of an increased number of targets including genetic variation [26] or pathogens [27]. However, multiplex dPCR has so far not been applied to the analysis of miRNAs, but would respond to the needs for implementation of miRNA-based signatures in clinical analysis. In the current study, we present a novel strategy to analyse multiple miRNAs simultaneously by dPCR, evaluate parameters influencing the performance of the assay and enable adjustment of read-out levels and show that miRNAs can be reproducibly quantified.

2. Material and methods

The optimisation of the different parameters is described in detail in the results section. In this paragraph the final optimised protocol is presented. The Minimum Information for Publication of Quantitative Digital PCR Experiments (dMIQE) checklist [28] ensuring reproducible and high-quality dPCR experiments is available in the Supplemental section (Supplemental Table 1). Of note, not all sections are relevant for this technology development.

2.1. Synthetic samples

Synthetic miRNAs and templates corresponding to the reverse transcription (RT) products (complementary DNA (cDNA) sequence) were ordered from Integrated DNA Technologies (IDT, Leuven, Belgium) or Eurogentec (Seraing, Belgium). Sequences are given in Supplemental Table 2.

2.2. Biological resources

The human THP-1 cell line (ATCC, TIB-202 lot 63176297, Manassas, VA, USA) was used as a model system for the implementation of the multiplex dPCR assay. Cells were maintained in RPMI 1640 plus L-glutamine medium (Gibco Life Technologies, #21875034, Villebon sur Yvette, France) complemented with antibiotics 100 units/mL penicillin and 100 µg/mL streptomycin (Gibco Life Technologies, #15140122, Villebon sur Yvette, France), 0.05 mM 2-mercaptoethanol (Gibco Life Technologies, #31350010, Villebon sur Yvette, France) and 10 % foetal bovine serum (Gibco Life Technologies, #A5670701, Villebon sur Yvette, France) at 37 °C in a 5 % CO_2 atmosphere. THP-1 cells were subcultured in suspension every 2–3 days until passage ($p < 10$). Total RNA and the smallRNA-enriched fraction were extracted from the cells using the RNeasy MinElute Cleanup Kit (Qiagen, #74204, Courtaboeuf, France) and the miRNeasy Mini Kit (Qiagen, #217004, Courtaboeuf, France) according to the manufacturer's instructions. Concentrations were measured on a Nanodrop (Thermo Fisher Scientific, Wilmington, DE, USA) and samples were diluted at 2 ng/µL.

Enriched small RNA fractions were also obtained using the same procedure from monocytes ($CD14^+$) from anonymized blood samples collected by the French Blood Donor Bank (Etablissement Français du Sang (EFS), Rungis, France) as previously described [29]. Briefly,

peripheral blood mononuclear cells were isolated by a Ficoll density gradient using UNISEP Maxi + tubes (Eurobio Scientific, # U-10, Les Ulis, France). Monocytes were then positively sorted by $CD14^+$ magnetic beads on a magnetic column, according to the manufacturer's instructions (Miltenyi Biotech, # 130-042-201, Paris, France).

2.3. Selection of miRNAs

For this proof-of-concept six miRNAs (hsa-let-7a-5p, hsa-miR-140-5p, hsa-miR-107, mir140, miR-335-5p, hsa-miR-23b-3p and hsa-miR-223-5p) known to be expressed in the human monocytic THP-1 cell line were randomly selected regardless of any biological function.

2.4. Primer and probe design

Primers and probes were designed following the recommendations of a previously reported qPCR protocol for miRNA analysis [30]. The stem-loop sequence, shown in Supplemental Fig. 1 and Supplemental Table 2, was first reported by Chen et al., allows for the specific capture of mature miRNAs and covers an expression range of 7 logs [31]. This stem-loop primer has been used in many research studies and in the commercially available standard TaqMan miRNA assays (Thermo Fisher Scientific) [5,32–35]. Six nucleotides reverse complementary to the 3' end of each miRNA were added as recommended in Ref. [30] to the published stem-loop sequence to generate the miRNA-specific stem-loop primers (Fig. 1 and Supplemental Fig. 1).

Forward dPCR primers were designed by adding 4 to 6 nucleotides to 5′ end of the mature miRNA sequence to reach an appropriate melting temperature (61–64 °C). Melting temperature, secondary structures and self-dimers and heterodimers were assessed with the OligoAnalyzer™ Tool (IDT, https://eu.idtdna.com/calc/analyzer, Leuven, Belgium). For the universal reverse primer, the previously published sequence [30] as well as a shortened version, removing the first three bases from the 5′-end (5′-GTGCAGGGTCCGAGGTA-3′), were evaluated. The shortened version was investigated to differentiate its melting temperature from the one of the hydrolysis probes (70 °C). Probe sequences (reverse PCR strand) labelled with a quencher and fluorophore were designed to cover the junction between the mature miRNA and the stem-loop primer avoiding overlap with the forward primer (Fig. 1 and Supplemental Fig. 1). Three to four LNA bases, preferably on the mature miRNA sequence, were added to the probe sequence to increase specificity and melting temperature. Among the fluorophores and quenchers recommended by the manufacturer for each fluorescent channel, the most commonly used were chosen for cost effectiveness. Selected combinations were: 6-Fluorescein amidite (FAM)/Black Hole Quencher (BHQ) 1® or Iowa Black® FQ for the blue channel, Cyanine3 (Cy3)/Iowa Black® FQ (IABkFQ) or ATTO 550/BHQ-2® for the green channel, Cyanine5 (Cy5)/Iowa Black® RQ (IAbRQSp) for the red channel, ROX (carboxy-X-rhodamine)/BHQ-2® for the yellow channel, ATTO 700/BHQ-3® for the infrared channel and Yakima Yellow®/BHQ-1® or Tetrachlorofluorescein (TET)/BHQ-1® for the teal channel. All primers, probes and miRNA sequences are shown in Supplemental Table 2 and their relative positioning on the mature miRNA sequences is shown in Supplemental Fig. 1.

2.5. RT-qPCR

Reverse transcription with a single stem-loop primer was performed with the Taqman MicroRNA RT kit (Thermo Fisher Scientific, #10146854, Villebon sur Yvette, France) with the following recommended protocol: 0.15 µL of 100 nM dNTP, 1 µL of MultiScribe™ reverse transcriptase (50 U/µL), 1.5 µL of 10× reverse transcription buffer, 0.19 µL of RNAse inhibitor (20 U/µL) and 4.16 µL of nuclease-free water mixed with 5 µL of the miRNA at 0.066 µM. Then 3 µL of the stem-loop primer (250 nM) were added and reverse transcription was performed in a thermocycler with an incubation step at 16 °C for 30 min followed by incubation at 42 °C for 30 min. The reaction was stopped by heating the mixture for 5 min at 85 °C prior to a final hold at 4 °C.

qPCR gradients of the annealing temperature (58 °C–68 °C) were performed on a LightCycler 96 gradient (Roche, #05 815,916,001) with the KAPA SYBR® FAST LC480 kit (Sigma-Aldrich, #KK4610, Saint-Quentin-Fallavier, France) by mixing 2 µL of the RT product of let7a, miR-140 and miR-107 or 2 µL of the respective synthetic template, at 0.02 µM, with 0.4 µL of both forward and reverse primers (10 µM), 10 µL of Master Mix 2X and water to a final volume of 20 µL. qPCR was performed in a 96-well plate on a LightCycler 480 (Roche, # 05015278001, Meylan, France) with the following program: pre-incubation at 95 °C for 3 min, 45 cycles of amplification at 95 °C for 10 s, a gradient for the annealing temperature between 58 °C and 68 °C for 20 s and 72 °C for 1 s, melting curve at 95 °C for 5 s, 65 °C for 1 min, heating to 97 °C with

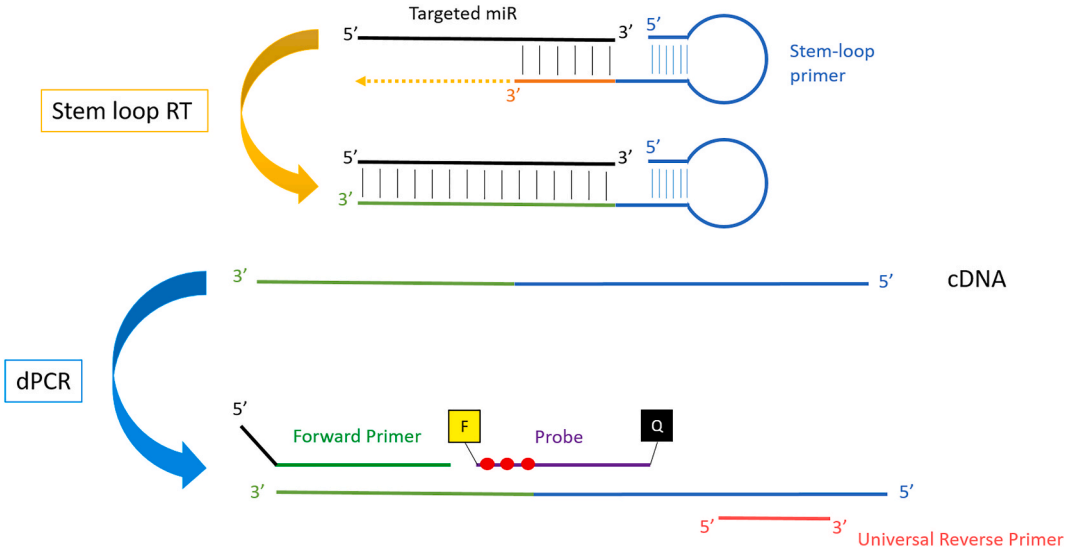

Figure 1. Schematic overview of the developed workflow including the stem-loop reverse transcription (RT) and dPCR reactions. In the RT reaction, cDNA is synthesized after the stem-loop primer hybridizes to the targeted miRNA with its 3′ end complementary to the 3′ end of the miRNA sequence. In the dPCR reaction, a forward primer specific for the 5′ part of the cDNA and a universal reverse primer complementary to the stem-loop part is used. A hydrolysis probe containing locked nucleic acids (symbolized as red dots on the probe) with a fluorescent dye and quencher covers both the 3′ end of the miRNA sequence and the stem-loop sequence.

5–10 acquisitions/°C, then cooling at 40 °C for 10 s.

PCR efficacy was tested with the same KAPA kit on a 12-point dilution series (2-fold dilutions) using a synthetic template (0.02 μM), the RT product of 0.33 pmol of the respective miRNAs or 10 ng of random miRNAs. Total RNA extracted from the THP-1 cell line (0.67 ng/μL) was also tested with and without an RT reaction. The size of the amplification product was verified on a LabChip GX (Revvity, #P231106106, Bussy Saint Martin, France).

2.6. Multiplex reverse transcription

A pool of all the RT stem-loop primers was made by mixing 10 μL of each primer (2.5 μM except for the primer for miR-140 which was at 250 nM) in Tris-EDTA (pH = 8.0, Sigma-Aldrich #93283, Saint-Quentin-Fallavier, France) in a final volume of 1 mL. The final concentration for each primer was accordingly 25 nM and 2.5 nM for miR-140. To facilitate the formation of the stem-loop structure, an aliquot of the RT primer pool was incubated at 95 °C, 80 °C, 70 °C, 60 °C, 50 °C, 40 °C, 30 °C and 20 °C for 30 s at each temperature.

The same TaqMan MicroRNA RT kit (Thermo Fisher Scientific, #10146854, Villebon sur Yvette, France) was used according to manufacturer's instructions with some adjustements: the RT mix consisted of 6 μL of stem-loop-primer pool, 0.3 μL of 100 mM dNTPs (with dTTP), 3 μL of MultiScribe™ reverse transcriptase (50 U/μL), 1.5 μL of 10X reverse transcription buffer, 0.19 μL of RNase inhibitor (20 U/μL) and 1 μL of nuclease-free water. After mixing gently all reagent on ice (no vortex) and a brief spin down, 3 μL of the sample was added. The reaction was incubated for 5 min on ice. Reverse transcription was then performed with the same program as described in 2.5.

2.7. Digital PCR (dPCR)

2.7.1. Sapphire chips

Primers (six forward and the universal reverse primer) were each diluted to 25 μM and pooled together at equimolar concentrations (pool concentration: 25 μM total and 3.57 μM for each of the seven primers). Probes were diluted to obtain a 6.25 μM solution and then pooled together equivalently (pool concentration: 6.25 μM total and 1.04 μM each).

A 25 μL dPCR mix was prepared with the naica® multiplex PCR MIX 5X (Stilla Technologies, #R10054, Villejuif, France) by mixing 9 μL of nuclease-free water, 5 μL of Buffer A, 4 μL of the primer pool (final concentration: 4 μM total, 0.57 μM each), 2 μL of the probe pool (final concentration: 500 nM, 83 nM each) and 5 μL of the RT mix or the synthetic template (2 fM each cDNA, 0.33 fM when pooled).

Sapphire chips (Stilla Technologies, #C14012, Villejuif, France) were prepared according to the manufacturer's instructions and loaded into the Geode of the naica® system (Stilla Technologies, #H15000, Villejuif, France) for partitioning and amplification using the following program: partition at 40 °C for Sapphire V1 followed by denaturation at 95 °C for 10 min, 55 cycles (unless otherwise specified) of 95 °C for 30 s and 60 °C for 1 min followed by the release pressure program for Sapphire V1.

Chips were scanned on a Prism6 scanner (naica® system, Stilla Technologies, #H24000.6, Villejuif, France) with the Crystal Reader software (Stilla Technologies, version 3.1.6.3, Villejuif, France) using the default template "ScanningTemplate_Prism6_SapphireChip_naica-multiplex-PCR-MIX_Taqman_v1.4" and results were analysed with Crystal Miner software (Stilla Technologies, version 3.1.6.3, Villejuif, France). To correct spill-over, an assay-specific compensation matrix was computed with Crystal Miner using monocolour controls analysing the six synthetic miRNAs separately and a negative control. This matrix was applied to all further experiments analysing the same targets. The relative uncertainty of the Poisson law was calculated by the Crystal Miner software for each sample. The Limit of Blank (LoB) for the six assays was estimated as the 95th percentile based on the concentration from 24 negative controls (no input in the RT). The limit of detection (LOD) for each assay was calculated with the formula LOD = 3.3 *σ/S where σ is the standard deviation of the same 24 negative controls and S is the slope of the calibration curve.

2.7.2. Ruby chips

The same protocol as for the Sapphire chips with the same buffer, primer and probe concentrations was used for the loading of the Ruby chips (Stilla Technologies, #C16011, Villejuif, France) with the exception of a reduced final reaction volume of 5 μL instead of 25 μL. Ruby chips were prepared according to the manufacturer's instructions and loaded into the Geode of the naica® system for partitioning and amplification using the following program: partition at 25 °C for Ruby V1 followed by denaturation at 95 °C for 10 min, 55 cycles of 95 °C for 30 s and 60 °C for 1 min followed by the release pressure program for Ruby V1. Chips were scanned on a Prism6 scanner with the default template "ScanningTemplate_Prism6_RubyChip_naica-multiplex-PCR-MIX_Taqman_v1.1".

3. Results

3.1. Design

We evaluated different designs for the set-up of probe-based dPCR assays including ligation-based approaches, polyA-tailing and stem-loop primers. A design based on a stem-loop was chosen due to its flexibility to place the primers and probes on the limited space available and avoid any biases due to ligation. Assays were designed to have a miRNA-specific forward primer with an estimated melting temperature of approximatively 62 °C for the amplification and a higher melting temperature of around 70 °C for the probe, obtained by incorporating three to four LNA bases.

3.2. Development

3.2.1. 1-plex assay

We first focused our development on three miRNAs (let7a-5p, miR-140b-5p, miR-107). The reverse transcription (RT) reaction for each of the three miRNAs was performed separately with the respective stem-loop primers. After RT, an amplification product of the expected size was detected by capillary electrophoresis on a LabChip GX instrument demonstrating the feasibility of the first step of our protocol (data not shown). We then tested the amplification efficiency by qPCR using two different universal reverse primers (Supplemental Table S2) corresponding to the primer proposed by Kramer et al. [30] as well as a shortened version removing three bases from the 5′ end to obtain a melting temperature comparable to the miRNA-specific forward primers. Amplification and melting curves for all three miRNA assays showed a more efficient amplification as well as the formation of a specific amplification product only for the shortened version of the reverse primer (Supplemental Fig. 2A). Reactions without a template did not yield an amplification product demonstrating the absence of interactions between the miRNA-specific forward primer and the stem-loop and/or the universal reverse primer (Supplemental Fig. 2B). Amplifications using either an RNA pool (THP-1) without prior RT or a random miRNA (5′-rNrNrNrNrNrNrNrNrNrNrNrNrNrNrNrNrNrNrN-3′) did not yield any amplification product suggesting specificity of the design (Supplemental Fig. 2B).

qPCR using a dilution series of a synthetic template corresponding to the RT product as well as the RT product showed high efficiency and linearity of the amplification (efficiency 1.9, correlation coefficient r^2 = 0.96 for the synthetic template and 2.2, r^2 = 0.99 for the RT product of let7a, Supplemental Fig. 3).

We rigorously investigated a number of technical parameters of the dPCR in a simplex reaction targeting let-7a using the synthetic template of the RT product. Prolonging the elongation time from 30 s to 1 min

improved separation of positive and negative droplets, as did the increase of the concentration of the forward miRNA-specific primer and the universal reverse primer from 1 to 2 μM (Supplemental Fig. 4A). On the other hand, reducing the denaturation time did not improve assay performance. The estimated annealing/elongation temperature of 60 °C yielded the best results as lowering the temperatures decreased separation between positive and negative droplets and higher temperature led to less positive droplets.

3.2.2. 3-plex assay

We then moved to a 3-plex assay using the same three miRNAs. Optimizing primer/probe concentrations and notably providing an equimolar mixture of all primers (forward and reverse) had little effect on the quantification of a synthetic template containing an estimated concentration of 1000 copies (cp)/μL/reaction (Fig. 2B), but had major effects on separability (Fig. 2A). The optimal concentrations for primer and probes were 1 μM for each primer and 166 nM for each probe in the reaction mixture, respectively. These concentrations were tested on three pools containing the three synthetic templates at a theoretical concentration of 100, 200 and 300 cp/μL yielding correlation coefficients above 0.95 (Fig. 2C). When the RT reaction was included in the workflow, the omission of the recommended naica® buffer (Buffer B) to the amplification reaction had a positive impact on droplet separation (Supplemental Fig. 4B).

3.2.3. 6-plex assay

Having demonstrated the feasibility of the simultaneous analysis of three miRNAs, we extended the analysis to a 6-plex assay targeting six miRNAs investigating the influence of a large number of parameters on the assay performance (Table 1).

In the course of adding three additional miRNAs, we changed the fluorophore for let7a and miR-335 evaluating both Yakima yellow and TET fluorophores. For let7a, TET was selected due to the larger fluorescent amplitude, while for miR-335 the change of the channel had a minor impact (Supplemental Fig. 4C). Using 1 pM (or 24,000 copies/μL) of each miRNA and 1 pM (4000 cp/μL) of a six-miRNA pool, a specific signal for each miRNA was obtained in the expected fluorescent channel (Fig. 3), while minimal signal was observed in the other channels except for the FAM channel where a higher background signal was observed.

We investigated the potential reason for this background by varying the concentration of the miRNA-specific forward primers as well as the concentration of the stem-loop (Supplemental Fig. 5). Overall, increasing the forward primers did not improve detection, but increased baseline and background noise. This was particularly true for the blue channel, in which the non-specific signal strongly increased when the concentration of the forward primers was doubled (Supplemental Fig. 5, negative control chamber 4 vs chamber 8). No effect was observed for the other five targeted miRNAs suggesting interactions between the miR-335 specific forward primer and the stem-loop primers. This was further supported by qPCR experiments on a dilution series and on the stem-loop primer pool alone without the addition of the targeted

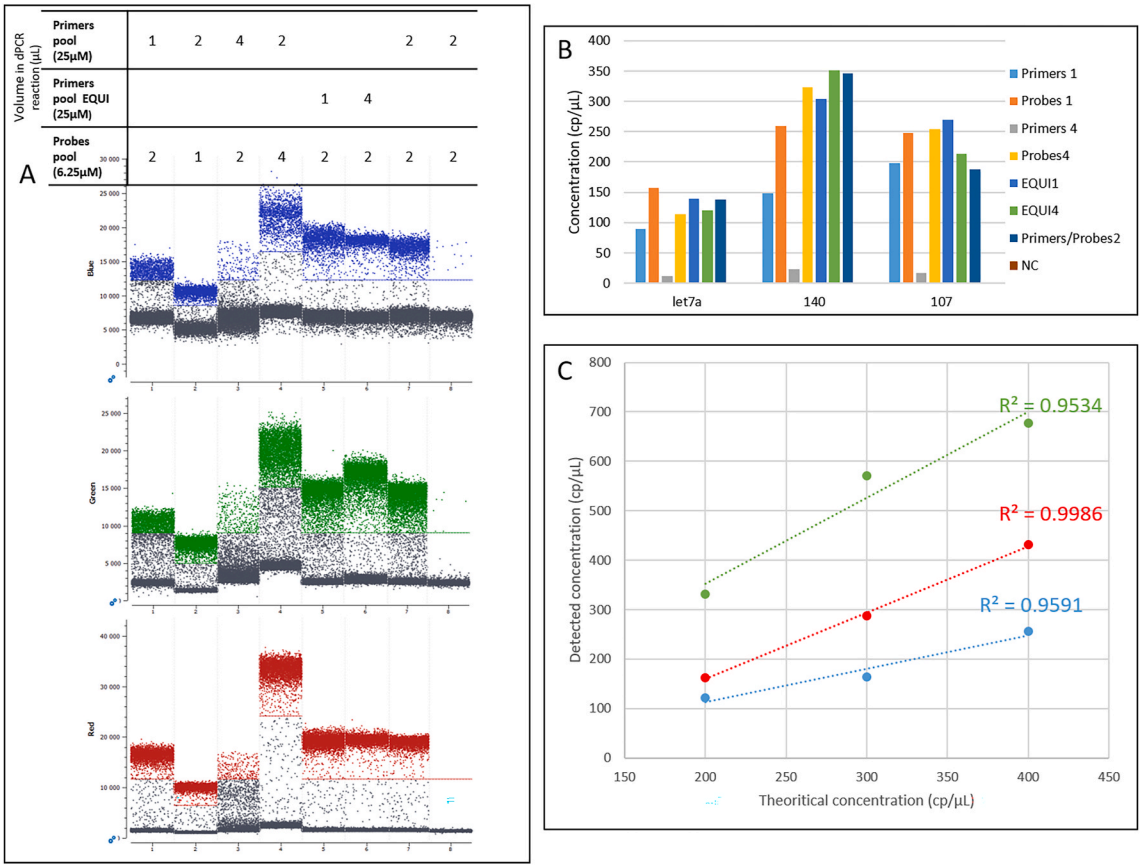

Fig. 2. Optimisation of primer and probe concentration (3-plex). The first primer pool (25 μM) contained three times more of the universal primer than the three forward primers (12.5 μM of the universal reverse primer and 4.16 μM of each forward primer). The second primer pool contained equimolar concentrations of all primers (6.25 μM each). Probe concentrations were constant (2.08 μM each). Volumes of the primer/probe pools used in this assay are detailed in the table above the dot plots in panel A. All chambers had a final concentration of 1X Buffer A and 4 % Buffer B and an input of 1000 cp/μL for each synthetic template except for the negative control (chamber 8). **A.** Uncompensated 1D dot plots of blue (let7a), green (miR-140) and red (miR-107) channels. **B.** Concentrations (cp/μL) obtained for the three targeted miRNAs. **C.** Linearity of the analysis of synthetic templates (with theoretical concentrations of 200, 300 and 400 cp/μL for each of the three templates under optimised conditions.

Table 1
Parameters tested and retained for the optimisation of the 6-plex assay.

Step	Parameter	Tested values/range	Retained value for the developed 6-plex	Justification for retained values	Ref
RT	Biological sample concentration (sorted cells)	0.5 -> 2 ng/µL	1 ng/µL	Good separability, sufficient number of positive droplets, no saturation.	Data not shown
	Biological sample concentration (cell line total RNA)	0.25 -> 42 ng/µL	2 ng/µL	Good separability, sufficient number of positive droplets, no saturation.	Data not shown
	Biological sample concentration (cell line enriched miRNA)	0.0035-> 2 ng/µL	0.07 ng/µL	Good separability, sufficient number of positive droplets, no saturation.	SFig. 7
	Final Stem-Loop Concentration	2.5 -> 400 nM	2.5 nM for miR-140 25 nM for the 5 others	1) 25 nM yields sufficient positive droplets and a low unspecific signal. 2) observed concentrations for miR-140 are comparable to the 5 other miRNAs when using 10 times less stem-loop primer.	Fig. 4CSFig. 5
	Inactivation step temperature	85/95 °C	85 °C	Less rain, better separability	Data not shown
dPCR mix	Concentration Primer Forward	0.05 -> 1.14 µM each	0.57 µM each (4 µM pool)	Low concentrations of forward primers do not lead to sufficient positive droplets (low signal). High concentrations of forward primers increase non-specific signal.	Data not shown Fig. 2A SFig. 4A SFig. 5
	Sequence and concentration Primer UR	Sequence from Ref. [30] and a shortened sequence	shortened sequence (CACGCATGAGGTAGTAGG)	Earlier amplification curves, sharper melting curves.	SFig. 1A
		0.05 -> 2 µM	0.57 µM (4 µM pool)	Low concentrations of reverse primers do not lead to sufficient positive droplets (low signal). High concentrations of reverse primers increase non-specific signal. Better separability with an equivalent concentration of reverse and forward primer.	Data not shown Fig. 2A S.Fig. 4A S. Fig. 5
	Teal fluorophore	Yakima Yellow, TET	TET	Better separability.	SFig. 4C
	Green fluorophore	Cy3, Atto550	Atto550	Better performance	Data not shown
	Buffer composition	With and without Buffer B	No buffer B with RT input	Better separability.	SFig. 4B
dPCR cycling	Denaturation time	15/30 s	30 s	Less dispersion of the baseline.	Data not shown
	Annealing temperature	58 -> 62 °C	60 °C	Better separability.	Data not shown
	Elongation time	15 s -> 1 min	1 min	Better separability.	Data not shown
	Number of cycles	45 -> 65	55	Better separability.	Data not shown
Scan	Exposure time in green	100/300 ms	100 ms	No improvement with 300 ms.	Data not shown

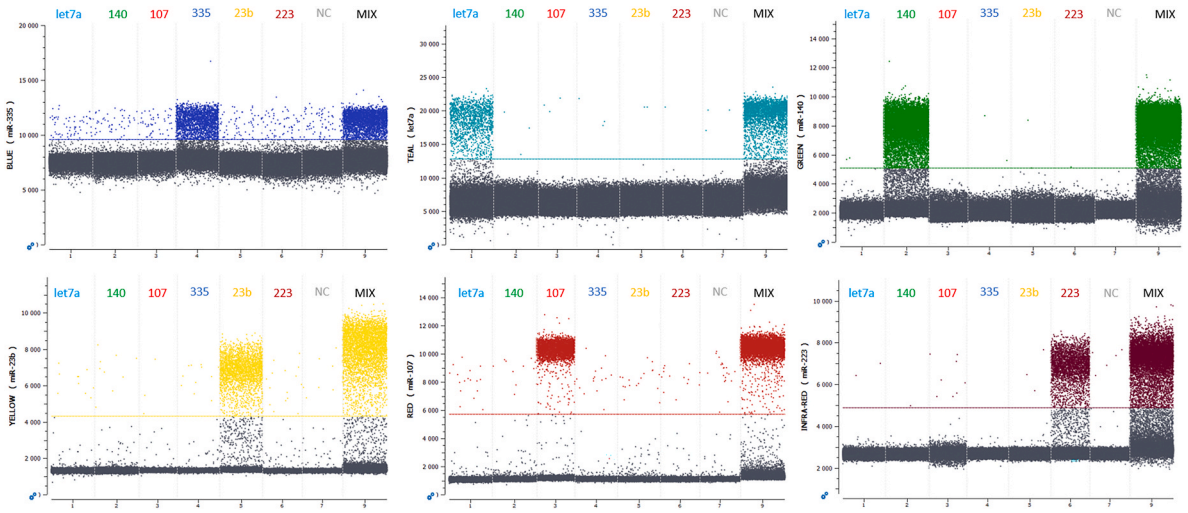

Fig. 3. Compensated 1D dot plots for the six channels of the 6-plex assay. RT input consisted of all six targeted synthetic miRNAs separately and mixed together. Chamber 1 to 6 contains the RT product of each miRNA (with a concentration of 24,000 cp/μL prior to RT in the dPCR mix). Chamber 7 is a negative control (no input in the RT). Chamber 8 contains the RT product of the six targeted synthetic miRNA pooled together (24,000 cp/μL global and 4000 cp/μL for each miRNA in the dPCR reaction).

miRNA. Stem-loop primers showed a threshold cycle (C_p) close to the negative control (water) for all the PCRs except for miR-335, for which amplification occurred within the dilution series, right before the 2 pM dilution curves. These results confirmed a higher background signal for miR-335 compared to the five other miRNAs, but still allowing quantification at higher concentrations. Due to the restricted size and resulting limited possibility to redesign miRNA assays targeting miR-335, we decided to continue the evaluation of this miRNA multiplex assay since this situation is likely to happen in the future when implementing a panel of clinical relevance and the target miRNA of a signature cannot be easily replaced.

Subsequently, the linearity of the dPCR reaction in the 6-plex reaction with a dilution series from 100,000 copies to 2500 copies for each miRNA template as input in the reverse transcription reaction was investigated. The results (Fig. 4A and B) showed a very high linearity between the different concentration for the respective miRNAs (R^2 = 0.898 to 0.999). However, the detected concentrations did not correspond to the expected number of copies per μL and there was some

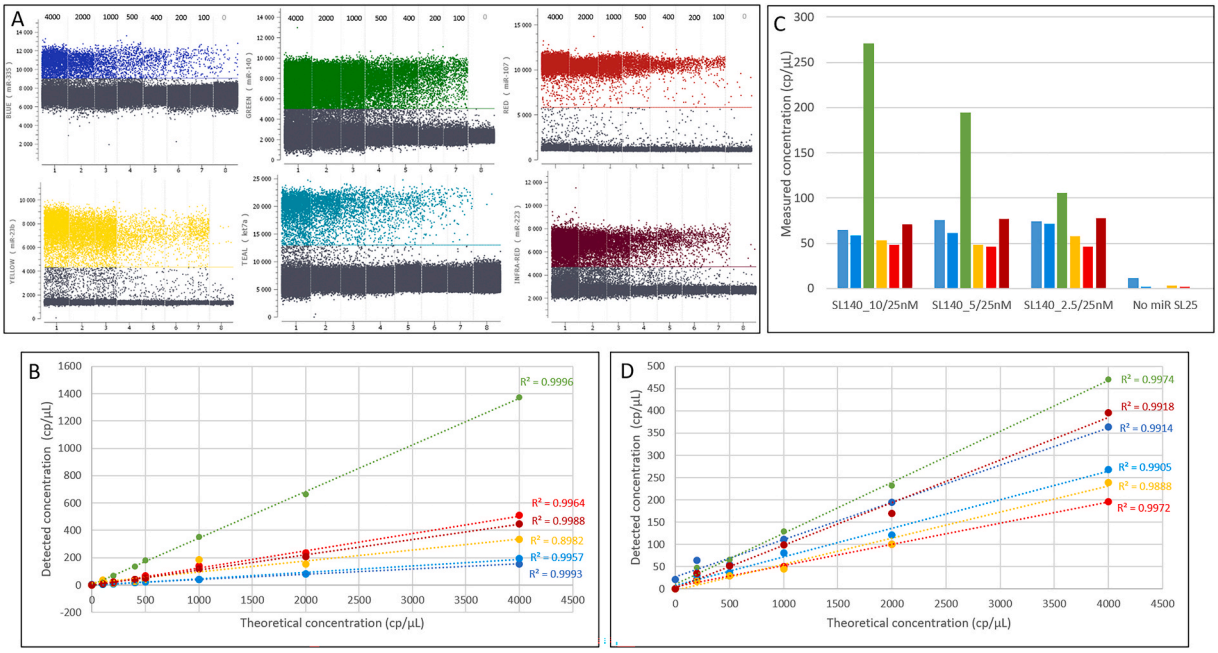

Figure 4. Linearity of a dilution series of a pool containing six synthetic miRNAs. **A.** Compensated 1D dot plots for the six channels. A solution from 1 pM to 25 fM (1, 0.5, 0.25 pM, 125, 100, 50, 25 fM) containing the six targeted miRNA (100,000; 50,000; 25,000; 12,500; 10,000; 5000; 2500 cp/μL each) was used for the RT reaction resulting in a final concentration of 4000; 2000; 1000; 500; 400; 200 and 100 cp/μL in the dPCR chambers. **B.** Dot plot for detected concentrations vs theoretical concentrations with linearity curves and coefficient of determination for the dilution series. The colour code corresponds to the fluorescent channels (panel A). **C.** Detected concentrations (cp/μL) for the six targeted synthetic miRNA with different concentrations (10, 5 and 2.5 nM) for the miR-140 specific stem-loop (SL) primer in the stem-loop pool. Concentration of all other stem-loop primers was kept constant (25 nM). **D.** Dot plot for detected concentrations vs theoretical concentrations with linearity curves and coefficient of determination in a dilution series with the new stem-loop pool concentration (2.5 nM for miR-140/25 nM for the other five miRNAs). The colour code corresponds to the fluorescent channels (panel A).

variability between the concentrations obtained for the different miRNAs suggesting a varying efficiency of the RT reaction. Particularly, miR-140 showed much higher copy numbers compared to the other miRNAs. We therefore tested if the assay could be adjusted to obtain values in a similar range compared to the other miRNAs. Decreasing the concentration (10 times) of the stem-loop primer for this miRNA led to comparable values for all miRNAs included in the multiplex assay (Fig. 4C) maintaining optimal linearity ($R^2 = 0.988$ to 0.997) (Fig. 4D). As the measured number of copies differed from the expected ones, we aimed at confirming that samples with varying proportions of the six miRNAs in pools could be accurately measured by the 6-plex assay and that the measured proportional changes did reflect the expected factors. Eight pools containing varying concentrations of each miRNA were tested (Supplemental Fig. 6). Results confirmed a high linearity ($R^2 = 0.902$ to 0.998) between the expected and detected concentrations demonstrating that the expression of miRNAs differing by a factor of two could be easily identified. The Limit of Blank (LoB) for the six assays was calculated as 30.73 cp/μL for miR-335, 0.75 cp/μL for miR-140, 3.51 cp/μL for miR-107, 1.76 cp/μL for let7a, 2.40 cp/μL for miR-23b and 1.91 cp/μL for miR-223. The limit of detection (LOD) for each assay was calculated with the calibration curve (Fig. 4D). Except for miR-335, which showed an elevated LOD at 367 cp/μL due to the high background, the other miRNAs had a low LOD: 80.19 cp/μL for miR-170, 58.6 cp/μL for let7a, 46.7 cp/μL for miR-23b, 20.6 cp/μL for miR-223 and down to 8 cp/μL for miR-140.

3.3. 6-plex dPCR on the THP-1 cell line and blood monocytes

To validate our approach in complex biological samples expressing multiple miRNAs and other small non-coding RNAs, the six miRNAs were analysed in the THP-1 cell line using either 6 ng of total RNA or 6 ng and 210 pg of enriched small RNA fraction. All six miRNAs were detected in all samples (Supplemental Fig. 7) with the enriched fraction being saturated for let7a with 6 ng input.

As a last proof-of-concept and reproducibility test, we analysed the enriched small RNA fraction isolated from blood monocytes of six individuals (Supplemental Fig. 8). The concentrations of the six miRNAs (Fig. 5A) were very similar between the three independent experiments with the coefficients of variation ranging from 2 % to 17 % (Fig. 5B). These variations can at least be partially explained by the relative uncertainty of the Poisson law, which was between 2.6 % and 11 % for the six assays as determined by the Crystal Miner Software. miR-107 and miR-223 were below the LoB for sample R8 (43 % and 68 % of uncertainty) and thus not included in analyses. Let7a was highly expressed in all samples and the signal was saturated (Supplemental Fig. 8).

To avoid this saturation problem, we tested a stem-loop pool with a 10-fold lower concentration of the let7a primer (2.5 nM instead of 25 nM) similar to the approach taken for miR-140. As shown in Supplemental Fig. 9A, the linearity of the 6 targeted miRNAs was preserved and the signal in the monocyte samples was no longer saturated (Supplemental Fig. 9B) and therefore quantifiable. When analysing three independent RT reactions using the revised assay, we obtained similar reproducibility for the monocyte samples (average coefficients of variation of 7 % for miR-335, 15 % for miR-140, 13 % for miR-107, 12 % for let7a, 10 % for miR-23b and 11 % for miR-223) and THP-1 cell line (coefficients of variation of 4 % for miR-335, 21 % for miR-140, 8 % for miR-107, 20 % for let7a, 20 % for miR-23b and 27 % for miR-223).

3.4. Increasing throughput for the 6-plex dPCR

To evaluate the scalability of our assay, the same dilution series containing the pool of the six targeted miRNAs (from 4000 to 50 cp/μL for the dPCR reaction, Fig. 6) in triplicate as well as the miRNA separately were tested on Ruby chips. This support allows for the analysis of 16 samples instead of 4, allowing the analysis of 48 samples in one run. A specific signal for each miRNA was obtained in the expected fluorescent channel (Supplemental Fig. 10) and even if the detected concentrations were again lower than expected, they showed good linearity ($R^2 = 0.91$ to 0.99) (Fig. 6).

We also tested one of the monocyte samples (with an independent RT reaction) and compared the concentrations to those obtained on the Sapphire chips. The correlation between the concentrations of the different miRNAs found on Ruby and Sapphire chips were very high ($R^2 = 0.97$). We obtained highly similar results for miR-335 (2 % difference in the quantification results), miR-140 (8 %), let7a (5 %) and miR-23b (12 %) and a slightly larger variation for the lowly expressed (<150 cp/μL) miRNAs (miR-107, 19 % and miR-223, 20 %).

4. Discussion

In this study, we present a multiplex dPCR assay allowing the simultaneous detection and quantification of six miRNAs. To the best of our knowledge, this is the first dPCR assay targeting such a high number of miRNAs simultaneously.

dPCR shows improved flexibility for the handling of variable numbers of samples, has a shorter time to results, which can be obtained at much lower cost, and does not require a bioinformatic infrastructure for data analysis and interpretation compared to next generation sequencing-based assays. The shorter time to results, lower cost and easier interpretation of the obtained results might be of special importance for timely clinical decision making when dynamically monitoring treatment response and/or disease progression [36,37]. On the other hand, dPCR can only analyse a limited number of targets and thus requires prior knowledge on targets and is not well suited for the discovery of novel biomarkers. dPCR assays show improved sensitivity and signal-to-noise ratio compared to qPCR-based assays and are less

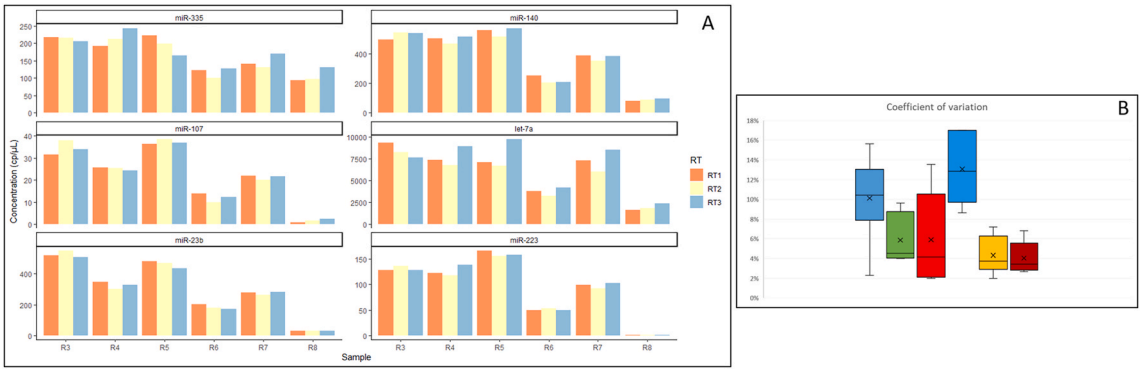

Figure 5. 6-plex assay reproducibility. **A**. Detected concentrations (cp/μL) for the six targeted miRNA in six blood samples for three separate RT reactions. **B.** Coefficient of variations for the six targeted miRNAs (without miR-107 and miR-223 for sample R8 due to very low concentrations).

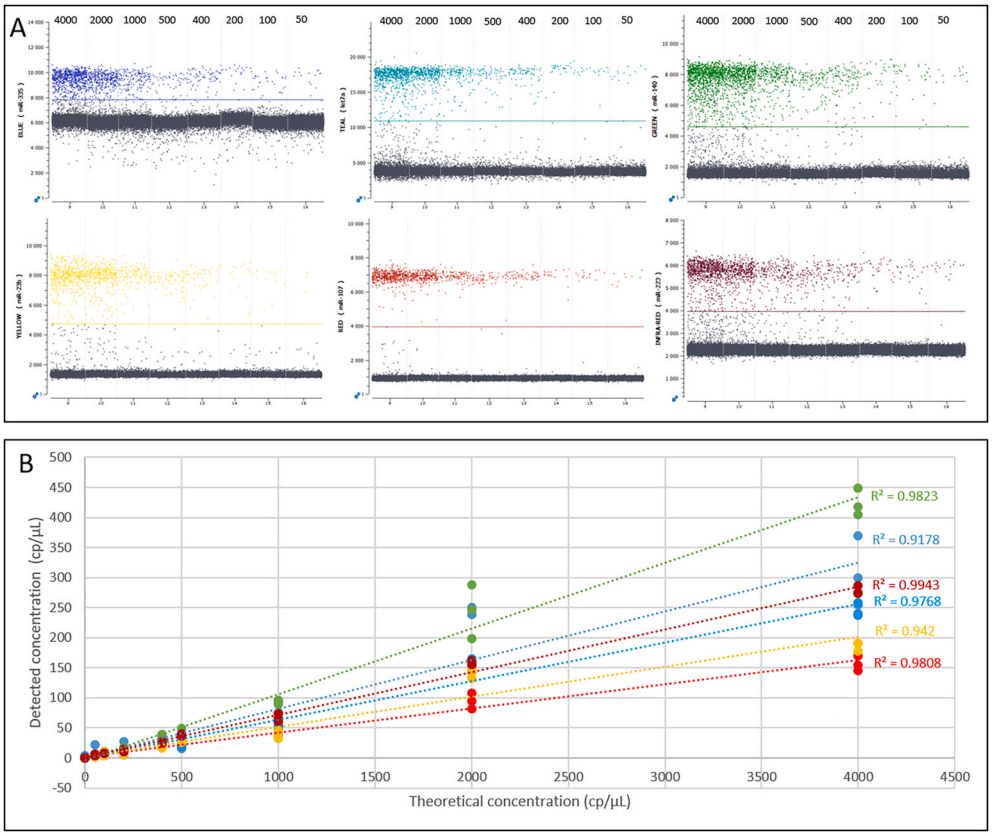

Fig. 6. 6-plex assay test using a high-throughput format (Ruby chip). **A.** Compensated 1D dot plots for the six channels for the dilution series (final concentrations of 4000 to 50 cp/µL). **B.** Dot plot for the detected concentrations vs theoretical concentrations with linearity curves and coefficient of determination. The colour code corresponds to the fluorescent channels (panel A).

susceptible to be influenced by PCR inhibitors [1,20,38]. dPCR has become a method of choice in laboratories performing clinical analyses, particularly mutation detection, detection of pathogens including COVID-19 and titration of vectors for gene therapy applications, but also DNA quantity and quality measures due to the relatively simple workflow and high sensitivity allowing to detect a specific signal against a large background [39–45].

Proof-of-concept studies have demonstrated the capacity of dPCR to accurately analyse miRNA including from liquid biopsies [19,46]. However, dPCR is not yet used in routine for miRNA analysis. This is at least partly due to the challenging design due to the limited size of the analyte, complexity of multiplexing with established technologies and the limitations on the biological material. Panels of miRNAs need to be analysed for most applications to achieve sufficient sensitivity and specificity requiring multiple reactions to be carried. For example, to determine the tissue of origin for metastatic cancer of unknown primary site, 13 reactions targeting a single miRNA were required [24]. While for the analysis of miRNAs from tumour tissue, the quantity of the required material is likely to be compatible with the analysis of multiple miRNAs, the required multiple parallel reactions will reduce the biological material available for other applications such as genetic profiling and pathological evaluation [24]. However, the quantity of miRNAs that can be obtained by non- or minimal invasive sampling from serum, plasma or other biofluids (liquid biopsy), is generally limited, especially if the miRNA content of exosomes and other extracellular vesicles is of interest. This precludes the analysis of a large number of miRNAs in parallel using qPCR-based assays. The implementation of multiplex dPCR assays addresses these challenges by including all targets in a single reaction, simplifying the workflow and limiting the required input.

An important advantage of our developed assay system is the possibility to switch between the Sapphire chips analysing four samples per chip and the Ruby chips analysing 16 samples per chip without the need for re-optimizing the reaction conditions. This will allow to develop the assay on the Sapphire chips and then perform routine analysis more cost-effectively on the Ruby chips. Analysis using the Ruby chips halves the cost per assay compared to the Sapphire chips, while allowing to analyse four times more samples in parallel and up to 144 samples on a working day. The flexibility might also be useful to adapt clinical applications to the number of samples that needs to be analysed reducing the time to results in case of need.

Intercalating dyes have been frequently used when only one or two miRNAs are targeted in an assay. The small size of miRNAs imposes significant challenges on the assay design, as it does not allow for the annealing of non-overlapping primers and a hydrolysis probe, which is mandatory for highly multiplexed miRNA assays. Three main strategies have been developed for increasing the size of the amplicon including ligation of primers/adaptors, polyadenylation of the mature miRNAs followed by a primer annealing partially to the poly-A tail or the use of stem-loop primers. Ligation based approaches are commonly used in sequencing-based approaches and have also been combined with dPCR [47]. However, ligation-based approaches are subject to a substantial bias depending on the type and sequence of the small RNA analysed and do not represent faithfully the distribution of miRNAs in the original biological sample [48].

Polyadenylation of miRNAs followed by amplification with a poly-T containing universal reverse primer as used in the miRCURY assays (Qiagen) has been shown in combination with LNAs to achieve high specificity [18]. This approach allows, at least in theory, for the amplification of all miRNAs with the same efficiency. However, due to the limited size of unique sequence, this design is difficult to use in combination with hydrolysis probes, which are a pre-requisite for multiplexing. The hydrolysis probe would partly overlap with the poly-A tail

and thus likely create unspecific signals due to the interaction with the poly-A tail of the different miRNAs. Furthermore, approaches based on poly-A tailing are unable to distinguish between mature miRNAs and pre-miRNAs.

The third approach, also used in the present study, uses thermostable stem-loop primers for the initial miRNA-specific reverse transcription step, creating an amplicon of sufficient size to place the two primers and the hydrolysis probe. While this approach significantly reduces the shortcomings associated with the other approaches, it should nonetheless be noted that each stem-loop primer has a specific 3′ end complementary to the targeted miRNA requiring thus a different stem-loop primer for each miRNA targeted. While this might be more costly during the optimisation phase than the other approaches, this cost is negligible for miRNA panels used on a large number of samples. The use of stem-loop primers reduces potential background from non-targeted and thus not amplified miRNAs. Stem-loop primers, similar to the one we use in the present study, are highly multiplexable analysing up to 220 miRNAs in a single cell [33]. In our study the designs were specific to the targeted miRNAs and no amplification was observed when the target miRNA was omitted from the analyses (Fig. 3, Supplemental Fig. 10). A pool of random miRNA sequences did also not show any unspecific amplification. Nonetheless, the potential cross-reactivity and non-specific amplification remains to be investigated in more detail for miRNAs with high sequence homology as well as in the presence of several isoforms of a miRNA of interest (isomiRs). Stem-loop based primers have been reported to not discriminate sufficiently between sequence variation at the 3' end [49].

One of the major advantages of dPCR is its ability for absolute quantification of some target molecules such as genetic variation or viral/bacterial sequences abolishing the need for calibration curves or standards [1]. Due to the presence of a single target molecule in each droplet, PCR efficiency biases are eliminated. Here, we show that due to the necessity to incorporate a reverse transcription step, the capacity for precise absolute quantification is lost. However, relative quantification is achieved with high accuracy and linearity as demonstrated by the high correlation coefficients between the expected and measured concentrations of the miRNAs. Therefore, absolute quantification of miRNAs can be achieved through the establishment of standard curves for the miRNAs of interest. Nonetheless, as we observed approximately 12-times less copies/μL as expected, it will be important for clinical applications to include only miRNAs that are expressed at a sufficiently high level to be reliably detected (100 cp/μL) and that differ sufficiently for the phenotype of interest to ensure accurate discrimination. With a coefficient of variation not exceeding 30 % for the lowly expressed miRNAs, a 1.5-fold difference in expression should allow robust discrimination.

The high reproducibility between independent dPCR runs and RT reactions as shown in Fig. 5 will allow establishing the standard curves once for an assay panel and its further use for calculating absolute copy numbers/μL of the samples. It should be pointed out that the expected concentration of the miRNAs is based on the concentration provided by the oligonucleotide supplier and there is currently no method available that would allow us to determine the actual concentration more accurately.

While in the present study we have targeted six different miRNAs expressed in the THP-1 cell line, the addition of one or several reference miRNAs could be used to improve absolute quantification. Normalisation strategies based on the global mean have been found to be most accurate for normalizing microRNA data [50], but are difficult to implement for dPCR due to the limited number of miRNAs that can be analysed. The choice of reference miRNAs will strongly depend on the tissue or cells targeted and widely used reference RNAs such as the small nuclear RNAs U6 or U44 have been shown to display high variation and in many cases perform less well compared to endogenous RNAs highlighting the need for references from the same class of RNA molecules [51–53]. The use of the geometric mean of several endogenous RNAs as reference RNAs validated for the specific application of the dPCR multiplex assay would allow improved quantification, but probably require a separate assay to be performed. This assay could also contain other quality control measures such as a control for haemolysis for liquid biopsy samples, commonly measured by the ratio between miR-451 and miR-23a [54]. Specific exogenous miRNAs spiked in the reaction already during RNA extraction such as cel-39-3p would in addition allow correcting for technical issues and sample-dependent performance of the reactions with a single assay.

We also investigated the feasibility and reproducibility of our assay in biological samples. The six assays were optimised to perform similarly on the different miRNAs leading to similar levels of quantification. However, the assay targeting let7a led to a complete saturation of the respective fluorescent channel in the $CD14^{+}$ monocytes pointing to the need to take expression levels of the targeted miRNAs into account early during the assay development in the same type of samples that will be subsequently analysed. As demonstrated for miR-140 during the optimisation of the assay and let7a for the analysis of the samples, reducing the amount of the stem-loop primer is an easily applicable method to decrease the signal for this miRNA while the performance of the detection of the other miRNA remains unaffected. Increasing the signal by increasing the stem-loop primer concentration to some extent might therefore be a viable alternative for some assays (Supplemental Fig. 5). Adjusting the stem-loop concentration can therefore be used to modulate the measured concentration of the target miRNAs and further reduce the limited variability between the different miRNA assays (Fig. 4D). dPCR assays analysing mutations or quantifying viral sequences have demonstrated high interlaboratory reproducibility [55, 56]. The development and analysis of miRNA signatures and their translation into the clinics has been hampered by assay-inherent biases as well as variability in the collection and pre-analytical treatment of the samples, which can lead to an altered representation of the miRNAs in the sample [6,48]. Furthermore, different enzymes or commercial kits used for the RT step are likely to have an impact on the measured expression level as previously shown for gene expression analysis by dPCR [57]. To enhance interlaboratory reproducibility, it will be important to provide standard operating procedures for the pre-analytical treatment as well as define all reagents prior to the dPCR reaction.

While a very low background signal as determined by the LoB was obtained for most of the targeted assay (<4 cp/μL for 5 out of 6 targets), the miR-335 assay had a significantly higher background signal (33 cp/μL) probably due to some interactions of the forward primer with the stem-loop primer pool, although these interactions were considered to be rather weak during the verification phase of the design. The limits of detection were similar to those previously reported (50 cp/μL) [20] for simplex assays suggesting that the multiplexing has no influence on the sensitivity of the assays. The assay for miR-335 performed not optimally with a higher background signal compared to the other assays. For the current multiplex panel, we could have exchanged the miRNA for an assay with a lower signal in the negative control, but we aimed to evaluate the performance of such an assay on biological samples. For clinical applications it might not always be possible to replace a miRNA performing less well with another one having the same information content. Due to the limited size of miRNAs, there are little possibilities for a re-design. While we focussed on a single stem-loop primer backbone for the presented study, stem loop primers with a different sequence have been published [58] and might reduce the observed interactions. Another possibility would be to shorten the forward primer by one or two bases and reinforce annealing to the targeted miRNA through the inclusion of locked-nucleic acids as for the hydrolysis probes. Our results demonstrate that despite the slightly increased background, quantification remained accurate and reproducible allowing thus to include such assays in the multiplex panel.

It is therefore likely that higher multiplexing factors can be achieved allowing to further increase the number of targets that can be analysed

in parallel. As stated, the RT reaction can be performed on a high number of targeted miRNAs and is therefore not likely to present a bottleneck for multiplexing although the chances for undesired interactions between the probes, specific primers and the stem-loop primers increase with their number and need to be carefully evaluated. Previous work using a commercial assay with a stem-loop primer design showed that non-specific signal only increased when more than 16 RT primers were pooled [20]. Beyond the use of different probe concentrations for amplitude-based multiplexing, that is commonly used for analysing more than one target in the same fluorescent channel, the use of two or more different fluorophores with different emission intensities in the same channel presents an interesting alternative as exemplified in our study by the use of either TET or Yakima Yellow® in the Teal channel. These approaches have been successfully applied to other molecular targets [59] and are likely transferable to the analysis of miRNAs although the impact of increased multiplexing on sensitivity and specificity needs to be evaluated in detail as spectral overlap of the fluorophores will impact these parameters. In addition, photobleaching using a combination of photostable and photosensitive reporter fluorophores in the same channel [60], population specific reporter assays [61] and colour combination approaches have been recently devised enabling to increase the multiplexing level up to a 16-plex assay for a six-colour scanner [62]. By using two probes per target, each population can be revealed in two colours expanding the number of targets per assay detectable while maintaining a simple analysis framework. These approaches have been mainly devised for the analysis of somatic mutations, but are likely transferable to miRNA analysis. A large number of different approaches for the multiplex analysis of miRNAs have been devised using a variety of amplification and detection technologies [63]. Few of them have been combined with dPCR leaving ample space for future developments. However, simplicity of data acquisition and interpretation will be key for maintaining the required sensitivity and specificity of the developed assays for clinical applications.

In the future, we will apply our method to the development of miRNA signatures with potential clinical relevance that could assist in clinical decision making. Besides the analysis of miRNAs in tissue and cells, miRNAs as bioactive cargo of exosomes and other extracellular vesicles have been implicated in deciphering diverse pathophysiological conditions making them potential biomarkers and therapeutic targets for a variety of diseases [64]. While the miRNA content of extracellular vesicles can be analysed by smallRNA sequencing (e.g. [65]), targeted analyses by qPCR are hampered by the limited available quantity and abundance of the biomolecules in the samples. dPCR has proven to be well suited for miRNA analysis from extracellular vesicles [20,46] and multiplex miRNA assays will further increase its usefulness by enabling the analysis of several miRNAs simultaneously reducing the required quantity of biological material. The quantity of miRNAs we obtain from liquid biopsies is compatible with the use in dPCR allowing probably for several multiplex assays to be performed on each sample [65]. However, appropriate normalisation strategies accounting for the overall miRNA content of a sample will be required for the correct interpretation of the results especially for longitudinal studies with multiple samples over time.

5. Conclusions

miRNA signatures have great potential to contribute significantly to the diagnosis of disease, monitor treatment response or detect disease progression. However, current technologies are not well suited for the use in clinical routine. dPCR has become a widely used method for clinical applications such as analysis of somatic mutations and detection of viral sequences, but has been little used for miRNA analysis. The presented study represents a first proof-of-concept for the multiplexed analysis of miRNAs using multi-colour dPCR demonstrating its feasibility and applicability to clinical samples with high reproducibility. Translation of already developed signatures into the proposed assay format could facilitate their uptake and implementation in clinical laboratories. The presented assay is performed on commercial dPCR instrument and applies a frequently-used strategy for reverse transcription. The assay has a short time to results and interpretation of results is straightforward. The developed approach addresses thus an important technology gap in the analysis of miRNAs with many clinical applications.

CRediT authorship contribution statement

Florence Busato: Writing – review & editing, Writing – original draft, Validation, Methodology, Investigation. **Sylvain Ursuegui:** Writing – review & editing, Validation, Methodology, Investigation. **Jean-François Deleuze:** Writing – review & editing, Resources, Funding acquisition. **Jorg Tost:** Writing – review & editing, Writing – original draft, Supervision, Methodology, Conceptualization.

Declaration of competing interest

The authors declare the following financial interests/personal relationships which may be considered as potential competing interests:

Jorg Tost reports financial support was provided by French National Research Agency. Jean-Francois Deleuze reports financial support was provided by French National Research Agency. Sylvain Ursuegui reports a relationship with Stilla technologies that includes: employment. If there are other authors, they declare that they have no known competing financial interests or personal relationships that could have appeared to influence the work reported in this paper.

Acknowledgment

This work was supported by the France Génomique National infrastructure, funded as part of "Investissement d'Avenir" program managed by Agence Nationale pour la Recherche (contract ANR-10-INBS-09) and the institutional budget of the CNRGH.

Appendix A. Supplementary data

Supplementary data to this article can be found online at https://doi.org/10.1016/j.aca.2024.343440.

Data availability

Raw dPCR data will be made available on request.

References

[1] J.F. Huggett, S. Cowen, C.A. Foy, Considerations for digital PCR as an accurate molecular diagnostic tool, Clin. Chem. 61 (2015) 79–88, https://doi.org/10.1373/clinchem.2014.221366.
[2] A. Kozomara, M. Birgaoanu, S. Griffiths-Jones, miRBase: from microRNA sequences to function, Nucleic Acids Res. 47 (2019) D155–D162, https://doi.org/10.1093/nar/gky1141.
[3] K.K. Farh, A. Grimson, C. Jan, B.P. Lewis, W.K. Johnston, L.P. Lim, C.B. Burge, D. P. Bartel, The widespread impact of mammalian MicroRNAs on mRNA repression and evolution, Science 310 (2005) 1817–1821, https://doi.org/10.1126/science.1121158.
[4] L. Peiro-Chova, M. Pena-Chilet, J.A. Lopez-Guerrero, J.L. Garcia-Gimenez, E. Alonso-Yuste, O. Burgues, A. Lluch, J. Ferrer-Lozano, G. Ribas, High stability of microRNAs in tissue samples of compromised quality, Virchows Arch. 463 (2013) 765–774, https://doi.org/10.1007/s00428-013-1485-2.
[5] P.S. Mitchell, R.K. Parkin, E.M. Kroh, B.R. Fritz, S.K. Wyman, E.L. Pogosova-Agadjanyan, A. Peterson, J. Noteboom, K.C. O'Briant, A. Allen, D.W. Lin, N. Urban, C.W. Drescher, B.S. Knudsen, D.L. Stirewalt, R. Gentleman, R.L. Vessella, P. S. Nelson, D.B. Martin, M. Tewari, Circulating microRNAs as stable blood-based markers for cancer detection, Proc. Natl. Acad. Sci. USA 105 (2008) 10513–10518, https://doi.org/10.1073/pnas.0804549105.
[6] G.B. Andersen, J. Tost, Circulating miRNAs as biomarker in cancer, recent results, Cancer Res. 215 (2020) 277–298, https://doi.org/10.1007/978-3-030-26439-0_15.
[7] K. Nemeth, R. Bayraktar, M. Ferracin, G.A. Calin, Non-coding RNAs in disease: from mechanisms to therapeutics, Nat. Rev. Genet. 25 (2024) 211–232, https://doi.org/10.1038/s41576-023-00662-1.

[8] G. Sozzi, M. Boeri, M. Rossi, C. Verri, P. Suatoni, F. Bravi, L. Roz, D. Conte, M. Grassi, N. Sverzellati, A. Marchiano, E. Negri, C. La Vecchia, U. Pastorino, Clinical utility of a plasma-based miRNA signature classifier within computed tomography lung cancer screening: a correlative MILD trial study, J. Clin. Oncol. 32 (2014) 768–773, https://doi.org/10.1200/JCO.2013.50.4357.

[9] M. Bagnoli, S. Canevari, D. Califano, S. Losito, M.D. Maio, F. Raspagliesi, M. L. Carcangiu, G. Toffoli, E. Cecchin, R. Sorio, V. Canzonieri, D. Russo, G. Scognamiglio, G. Chiappetta, G. Baldassarre, D. Lorusso, G. Scambia, G. F. Zannoni, A. Savarese, M. Carosi, P. Scollo, E. Breda, V. Murgia, F. Perrone, S. Pignata, L. De Cecco, D. Mezzanzanica, g. Multicentre Italian Trials in Ovarian cancer translational, Development and validation of a microRNA-based signature (MiROvaR) to predict early relapse or progression of epithelial ovarian cancer: a cohort study, Lancet Oncol. 17 (2016) 1137–1146, https://doi.org/10.1016/S1470-2045(16)30108-5.

[10] B. Pardini, G. Ferrero, S. Tarallo, G. Gallo, A. Francavilla, N. Licheri, M. Trompetto, G. Clerico, C. Senore, S. Peyre, V. Vymetalkova, L. Vodickova, V. Liska, O. Vycital, M. Levy, P. Macinga, T. Hucl, E. Budinska, P. Vodicka, F. Cordero, A. Naccarati, A fecal MicroRNA signature by small RNA sequencing accurately distinguishes colorectal cancers: results from a multicenter study, Gastroenterology 165 (2023) 582–599, https://doi.org/10.1053/j.gastro.2023.05.037, e588.

[11] L. De Cecco, M. Bagnoli, P. Chiodini, S. Pignata, D. Mezzanzanica, Prognostic evidence of the miRNA-based ovarian cancer signature MiROvaR in independent datasets, Cancers 13 (2021), https://doi.org/10.3390/cancers13071544.

[12] A. Ditto, L. De Cecco, B. Paolini, P. Alberti, F. Martinelli, U. Leone Roberti Maggiore, G. Bogani, P. Chiodini, S. Pignata, A. Tomassetti, F. Raspagliesi, D. Mezzanzanica, M. Bagnoli, Validation of MiROvaR, a microRNA-based predictor of early relapse in early stage epithelial ovarian cancer as a new strategy to optimise patients' prognostic assessment, Eur. J. Cancer 161 (2022) 55–63, https://doi.org/10.1016/j.ejca.2021.11.003.

[13] U. Pastorino, M. Boeri, S. Sestini, F. Sabia, G. Milanese, M. Silva, P. Suatoni, C. Verri, A. Cantarutti, N. Sverzellati, G. Corrao, A. Marchiano, G. Sozzi, Baseline computed tomography screening and blood microRNA predict lung cancer risk and define adequate intervals in the BioMILD trial, Ann. Oncol. 33 (2022) 395–405, https://doi.org/10.1016/j.annonc.2022.01.008.

[14] M. Boeri, F. Sabia, R.E. Ledda, M. Balbi, P. Suatoni, M. Segale, A. Zanghi, A. Cantarutti, L. Rolli, C. Valsecchi, G. Corrao, A. Marchiano, U. Pastorino, G. Sozzi, Blood microRNA testing in participants with suspicious low-dose CT findings: follow-up of the BioMILD lung cancer screening trial, Lancet Reg Health Eur 46 (2024) 101070, https://doi.org/10.1016/j.lanepe.2024.101070.

[15] P. Laurent-Puig, M.L. Grisoni, V. Heinemann, F. Liebaert, D. Neureiter, A. Jung, F. Montestruc, Y. Gaston-Mathe, R. Thiebaut, S. Stintzing, Validation of miR-31-3p expression to predict cetuximab efficacy when used as first-line treatment in RAS wild-type metastatic colorectal cancer, Clin. Cancer Res. 25 (2019) 134–141, https://doi.org/10.1158/1078-0432.CCR-18-1324.

[16] P. Starlinger, H. Hackl, D. Pereyra, S. Skalicky, E. Geiger, M. Finsterbusch, D. Tamandl, C. Brostjan, T. Grunberger, M. Hackl, A. Assinger, Predicting postoperative liver dysfunction based on blood-derived MicroRNA signatures, Hepatology 69 (2019) 2636–2651, https://doi.org/10.1002/hep.30572.

[17] S.D. Finkelstein, J.W. Sistrunk, C. Malchoff, D.V. Thompson, G. Kumar, V. A. Timmaraju, B. Repko, A. Mireskandari, L.A. Evoy-Goodman, N.A. Massoll, M. A. Lupo, A retrospective evaluation of the diagnostic performance of an interdependent pairwise MicroRNA expression analysis with a mutation panel in indeterminate thyroid nodules, Thyroid 32 (2022) 1362–1371, https://doi.org/10.1089/thy.2022.0124.

[18] P. Mestdagh, N. Hartmann, L. Baeriswyl, D. Andreasen, N. Bernard, C. Chen, D. Cheo, P. D'Andrade, M. DeMayo, L. Dennis, S. Derveaux, Y. Feng, S. Fulmer-Smentek, B. Gerstmayer, J. Gouffon, C. Grimley, E. Lader, K.Y. Lee, S. Luo, P. Mouritzen, A. Narayanan, S. Patel, S. Peiffer, S. Ruberg, G. Schroth, D. Schuster, J.M. Shaffer, E.J. Shelton, S. Silveria, U. Ulmanella, V. Veeramachaneni, F. Staedtler, T. Peters, T. Guettouche, L. Wong, J. Vandesompele, Evaluation of quantitative miRNA expression platforms in the microRNA quality control (miRQC) study, Nat. Methods 11 (2014) 809–815, https://doi.org/10.1038/nmeth.3014.

[19] C.M. Hindson, J.R. Chevillet, H.A. Briggs, E.N. Gallichotte, I.K. Ruf, B.J. Hindson, R.L. Vessella, M. Tewari, Absolute quantification by droplet digital PCR versus analog real-time PCR, Nat. Methods 10 (2013) 1003–1005, https://doi.org/10.1038/nmeth.2633.

[20] C. Wang, Q. Ding, P. Plant, M. Basheer, C. Yang, E. Tawedrous, A. Krizova, C. Boulos, M. Farag, Y. Cheng, G.M. Yousef, Droplet digital PCR improves urinary exosomal miRNA detection compared to real-time PCR, Clin. Biochem. 67 (2019) 54–59, https://doi.org/10.1016/j.clinbiochem.2019.03.008.

[21] E. Miotto, E. Saccenti, L. Lupini, E. Callegari, M. Negrini, M. Ferracin, Quantification of circulating miRNAs by droplet digital PCR: comparison of EvaGreen- and TaqMan-based chemistries, Cancer Epidemiol. Biomarkers Prev. 23 (2014) 2638–2642, https://doi.org/10.1158/1055-9965.EPI-14-0503.

[22] S. Hedayat, L. Cascione, D. Cunningham, M. Schirripa, A. Lampis, J.C. Hahne, N. Tunariu, S.P. Hong, S. Marchetti, K. Khan, E. Fontana, V. Angerilli, M. Delrieux, D. Nava Rodrigues, L. Procaccio, S. Rao, D. Watkins, N. Starling, I. Chau, C. Braconi, N. Fotiadis, R. Begum, N. Guppy, L. Howell, M. Valenti, S. Cribbes, B. Kolozsvari, V. Kirkin, S. Lonardi, M. Ghidini, R. Passalacqua, R. Elghadi, L. Magnani, D.J. Pinato, F. Di Maggio, F. Ghelardi, E. Sottotetti, G. Vetere, P. Ciraci, G. Vlachogiannis, F. Pietrantonio, C. Cremolini, A. Cortellini, F. Loupakis, M. Fassan, N. Valeri, Circulating microRNA analysis in a prospective Co-clinical trial identifies MIR652-3p as a response biomarker and driver of Regorafenib Resistance mechanisms in colorectal cancer, Clin. Cancer Res. 30 (2024) 2140–2159, https://doi.org/10.1158/1078-0432.CCR-23-2748.

[23] L. Lirussi, D. Ayyildiz, Y. Liu, N.P. Montaldo, S. Carracedo, M.R. Aure, L. Jobert, X. Tekpli, J. Touma, T. Sauer, E. Dalla, V.N. Kristensen, J. Geisler, S. Piazza, G. Tell, H. Nilsen, A regulatory network comprising let-7 miRNA and SMUG1 is associated with good prognosis in ER+ breast tumours, Nucleic Acids Res. 50 (2022) 10449–10468, https://doi.org/10.1093/nar/gkac807.

[24] N. Laprovitera, M. Riefolo, E. Porcellini, G. Durante, I. Garajova, F. Vasuri, A. Aigelsreiter, N. Dandachi, G. Benvenuto, F. Agostinis, S. Sabbioni, I. Berindan Neagoe, C. Romualdi, A. Ardizzoni, D. Trere, M. Pichler, A. D'Errico, M. Ferracin, MicroRNA expression profiling with a droplet digital PCR assay enables molecular diagnosis and prognosis of cancers of unknown primary, Mol. Oncol. 15 (2021) 2732–2751, https://doi.org/10.1002/1878-0261.13026.

[25] D. Conte, C. Verri, C. Borzi, P. Suatoni, U. Pastorino, G. Sozzi, O. Fortunato, Novel method to detect microRNAs using chip-based QuantStudio 3D digital PCR, BMC Genom. 16 (2015) 849, https://doi.org/10.1186/s12864-015-2097-9.

[26] J. Corne, F. Le Du, V. Quillien, F. Godey, L. Robert, H. Bourien, A. Brunot, L. Crouzet, C. Perrin, C. Lefeuvre-Plesse, V. Dieras, T. De la Motte Rouge, Development of multiplex digital PCR assays for the detection of PIK3CA mutations in the plasma of metastatic breast cancer patients, Sci. Rep. 11 (2021) 17316, https://doi.org/10.1038/s41598-021-96644-6.

[27] J. Wu, B. Tang, Y. Qiu, R. Tan, J. Liu, J. Xia, J. Zhang, J. Huang, J. Qu, J. Sun, X. Wang, H. Qu, Clinical validation of a multiplex droplet digital PCR for diagnosing suspected bloodstream infections in ICU practice: a promising diagnostic tool, Crit. Care 26 (2022) 243, https://doi.org/10.1186/s13054-022-04116-8.

[28] d. Group, J.F. Huggett, The digital MIQE guidelines update: minimum information for publication of quantitative digital PCR experiments for 2020, Clin. Chem. 66 (2020) 1012–1029, https://doi.org/10.1093/clinchem/hvaa125.

[29] O. Fogel, A. Bugge Tinggaard, M. Fagny, N. Sigrist, E. Roche, L. Leclere, J. F. Deleuze, F. Batteux, M. Dougados, C. Miceli-Richard, J. Tost, Deregulation of microRNA expression in monocytes and CD4(+) T lymphocytes from patients with axial spondyloarthritis, Arthritis Res. Ther. 21 (2019) 51, https://doi.org/10.1186/s13075-019-1829-7.

[30] M.F. Kramer, Stem-loop RT-qPCR for miRNAs, Curr Protoc Mol Biol, Chapter 15 (2011), https://doi.org/10.1002/0471142727.mb1510s95. Unit 15 10.

[31] C. Chen, D.A. Ridzon, A.J. Broomer, Z. Zhou, D.H. Lee, J.T. Nguyen, M. Barbisin, N. L. Xu, V.R. Mahuvakar, M.R. Andersen, K.Q. Lao, K.J. Livak, K.J. Guegler, Real-time quantification of microRNAs by stem-loop RT-PCR, Nucleic Acids Res. 33 (2005) e179, https://doi.org/10.1093/nar/gni178.

[32] F. Tang, P. Hajkova, S.C. Barton, K. Lao, M.A. Surani, MicroRNA expression profiling of single whole embryonic stem cells, Nucleic Acids Res. 34 (2006) e9, https://doi.org/10.1093/nar/gnj009.

[33] F. Tang, P. Hajkova, S.C. Barton, D. O'Carroll, C. Lee, K. Lao, M.A. Surani, 220-plex microRNA expression profile of a single cell, Nat. Protoc. 1 (2006) 1154–1159, https://doi.org/10.1038/nprot.2006.161.

[34] L. He, X. He, L.P. Lim, E. de Stanchina, Z. Xuan, Y. Liang, W. Xue, L. Zender, J. Magnus, D. Ridzon, A.L. Jackson, P.S. Linsley, C. Chen, S.W. Lowe, M.A. Cleary, G.J. Hannon, A microRNA component of the p53 tumour suppressor network, Nature 447 (2007) 1130–1134, https://doi.org/10.1038/nature05939.

[35] L. Shi, W. Zhu, Y. Huang, L. Zhuo, S. Wang, S. Chen, B. Zhang, B. Ke, Cancer-associated fibroblast-derived exosomal microRNA-20a suppresses the PTEN/PI3K-AKT pathway to promote the progression and chemoresistance of non-small cell lung cancer, Clin. Transl. Med. 12 (2022) e989, https://doi.org/10.1002/ctm2.989.

[36] C.M. Wood-Bouwens, D. Haslem, B. Moulton, A.F. Almeda, H. Lee, G.M. Heestand, L.D. Nadauld, H.P. Ji, Therapeutic monitoring of circulating DNA mutations in metastatic cancer with personalized digital PCR, J. Mol. Diagn. 22 (2020) 247–261, https://doi.org/10.1016/j.jmoldx.2019.10.008.

[37] K. Lin, Y. Zhao, B. Xu, S. Yu, Z. Fu, Y. Zhang, H. Wang, J. Song, M. Fan, Y. Zhou, J. Ai, C. Qiu, H. Zhang, W. Zhang, Clinical diagnostic performance of droplet digital PCR for suspected bloodstream infections, Microbiol. Spectr. 11 (2023) e0137822, https://doi.org/10.1128/spectrum.01378-22.

[38] T.C. Dingle, R.H. Sedlak, L. Cook, K.R. Jerome, Tolerance of droplet-digital PCR vs real-time quantitative PCR to inhibitory substances, Clin. Chem. 59 (2013) 1670–1672, https://doi.org/10.1373/clinchem.2013.211045.

[39] V. Taly, D. Pekin, L. Benhaim, S.K. Kotsopoulos, D. Le Corre, X. Li, I. Atochin, D. R. Link, A.D. Griffiths, K. Pallier, H. Blons, O. Bouche, B. Landi, J.B. Hutchison, P. Laurent-Puig, Multiplex picodroplet digital PCR to detect KRAS mutations in circulating DNA from the plasma of colorectal cancer patients, Clin. Chem. 59 (2013) 1722–1731, https://doi.org/10.1373/clinchem.2013.206359.

[40] S. Olmedillas-Lopez, R. Olivera-Salazar, M. Garcia-Arranz, D. Garcia-Olmo, Current and emerging applications of droplet digital PCR in oncology: an updated review, Mol. Diagn. Ther. 26 (2022) 61–87, https://doi.org/10.1007/s40291-021-00562-2.

[41] L. Hu, Y.Y. Ji, P. Zhu, R.Q. Lu, Mutation-Selected Amplification droplet digital PCR: a new single nucleotide variant detection assay for TP53(R249S) mutant in tumor and plasma samples, Anal. Chim. Acta 1318 (2024) 342929, https://doi.org/10.1016/j.aca.2024.342929.

[42] L. Sancha Dominguez, A. Cotos Suarez, M. Sanchez Ledesma, J.L. Munoz Bellido, Present and future applications of digital PCR in infectious diseases diagnosis, Diagnostics 14 (2024), https://doi.org/10.3390/diagnostics14090931.

[43] Y. Wang, S. Bergelson, M. Feschenko, Determination of lentiviral infectious titer by a novel droplet digital PCR method, Hum. Gene Ther. Methods 29 (2018) 96–103, https://doi.org/10.1089/hgtb.2017.198.

[44] D. Gleerup, Y. Chen, W. Van Snippenberg, C. Valcke, O. Thas, W. Trypsteen, W. De Spiegelaere, Measuring DNA quality by digital PCR using probability calculations,

Anal. Chim. Acta 1279 (2023) 341822, https://doi.org/10.1016/j.aca.2023.341822.
[45] A. Devonshire, G. Jones, A.F. Gonzalez, O. Kofanova, J. Trouet, P. Pinzani, S. Gelmini, S. Bonin, C. Foy, Interlaboratory evaluation of quality control methods for circulating cell-free DNA extraction, N. Biotech. 78 (2023) 13–21, https://doi.org/10.1016/j.nbt.2023.09.005.
[46] J.H. Bahn, Q. Zhang, F. Li, T.M. Chan, X. Lin, Y. Kim, D.T. Wong, X. Xiao, The landscape of microRNA, Piwi-interacting RNA, and circular RNA in human saliva, Clin. Chem. 61 (2015) 221–230, https://doi.org/10.1373/clinchem.2014.230433.
[47] H. Tian, Y. Sun, C. Liu, X. Duan, W. Tang, Z. Li, Precise quantitation of MicroRNA in a single cell with droplet digital PCR based on ligation reaction, Anal. Chem. 88 (2016) 11384–11389, https://doi.org/10.1021/acs.analchem.6b01225.
[48] M. Meistertzheim, T. Fehlmann, F. Drews, M. Pirritano, G. Gasparoni, A. Keller, M. Simon, Comparative analysis of biochemical biases by ligation- and template-switch-based small RNA library preparation protocols, Clin. Chem. 65 (2019) 1581–1591, https://doi.org/10.1373/clinchem.2019.305045.
[49] A. Schamberger, T.I. Orban, 3' IsomiR species and DNA contamination influence reliable quantification of microRNAs by stem-loop quantitative PCR, PLoS One 9 (2014) e106315, https://doi.org/10.1371/journal.pone.0106315.
[50] P. Mestdagh, P. Van Vlierberghe, A. De Weer, D. Muth, F. Westermann, F. Speleman, J. Vandesompele, A novel and universal method for microRNA RT-qPCR data normalization, Genome Biol. 10 (2009) R64, https://doi.org/10.1186/gb-2009-10-6-r64.
[51] H.J. Peltier, G.J. Latham, Normalization of microRNA expression levels in quantitative RT-PCR assays: identification of suitable reference RNA targets in normal and cancerous human solid tissues, RNA 14 (2008) 844–852, https://doi.org/10.1261/rna.939908.
[52] M.K. Das, R. Andreassen, T.B. Haugen, K. Furu, Identification of endogenous controls for use in miRNA quantification in human cancer cell lines, Cancer Genomics Proteomics 13 (2016) 63–68.
[53] H. Schwarzenbach, A.M. da Silva, G. Calin, K. Pantel, Data normalization strategies for MicroRNA quantification, Clin. Chem. 61 (2015) 1333–1342, https://doi.org/10.1373/clinchem.2015.239459.
[54] T. Blondal, S. Jensby Nielsen, A. Baker, D. Andreasen, P. Mouritzen, M. Wrang Teilum, I.K. Dahlsveen, Assessing sample and miRNA profile quality in serum and plasma or other biofluids, Methods 59 (2013) S1–S6, https://doi.org/10.1016/j.ymeth.2012.09.015.
[55] A.S. Whale, A.S. Devonshire, G. Karlin-Neumann, J. Regan, L. Javier, S. Cowen, A. Fernandez-Gonzalez, G.M. Jones, N. Redshaw, J. Beck, A.W. Berger, V. Combaret, N. Dahl Kjersgaard, L. Davis, F. Fina, T. Forshew, R. Fredslund Andersen, S. Galbiati, A. Gonzalez Hernandez, C.A. Haynes, F. Janku, R. Lacave, J. Lee, V. Mistry, A. Pender, A. Pradines, C. Proudhon, L.H. Saal, E. Stieglitz, B. Ulrich, C.A. Foy, H. Parkes, S. Tzonev, J.F. Huggett, International interlaboratory digital PCR study demonstrating high reproducibility for the measurement of a rare sequence variant, Anal. Chem. 89 (2017) 1724–1733, https://doi.org/10.1021/acs.analchem.6b03980.
[56] J. Pavsic, A. Devonshire, A. Blejec, C.A. Foy, F. Van Heuverswyn, G.M. Jones, H. Schimmel, J. Zel, J.F. Huggett, N. Redshaw, M. Karczmarczyk, E. Mozioglu, S. Akyurek, M. Akgoz, M. Milavec, Inter-laboratory assessment of different digital PCR platforms for quantification of human cytomegalovirus DNA, Anal. Bioanal. Chem. 409 (2017) 2601–2614, https://doi.org/10.1007/s00216-017-0206-0.
[57] R. Sanders, D.J. Mason, C.A. Foy, J.F. Huggett, Evaluation of digital PCR for absolute RNA quantification, PLoS One 8 (2013) e75296, https://doi.org/10.1371/journal.pone.0075296.
[58] Y. Cao, F. Zhao, P. Feng, Y. Hong, Y. Zhang, Z. Zhang, Y. Zhu, X. Song, Stem-loop RT-qPCR system for multiplex miRNA profiling and its application in wound healing-specific biomarker identification, Anal. Biochem. 678 (2023) 115267, https://doi.org/10.1016/j.ab.2023.115267.
[59] A.S. Whale, J.F. Huggett, S. Tzonev, Fundamentals of multiplexing with digital PCR, Biomol Detect Quantif 10 (2016) 15–23, https://doi.org/10.1016/j.bdq.2016.05.002.
[60] F. Schlenker, E. Kipf, N. Borst, T. Hutzenlaub, R. Zengerle, F. von Stetten, P. Juelg, Virtual fluorescence color channels by selective photobleaching in digital PCR applied to the quantification of KRAS point mutations, Anal. Chem. 93 (2021) 10538–10545, https://doi.org/10.1021/acs.analchem.1c01488.
[61] S. Calabrese, A.M. Markl, M. Neugebauer, S.J. Krauth, N. Borst, F. von Stetten, M. Lehnert, Reporter emission multiplexing in digital PCRs (REM-dPCRs): direct quantification of multiple target sequences per detection channel by population specific reporters, Analyst 148 (2023) 5243–5254, https://doi.org/10.1039/d3an00191a.
[62] I. Santos-Barriopedro, S. Ursuegui, E. Fradet, R. Dangle, Robust higher-order multiplexing in digital PCR by color-combination BioRxiv, preprint at, https://doi.org/10.1101/2023.05.10.540190, 2023.
[63] T. Jet, G. Gines, Y. Rondelez, V. Taly, Advances in multiplexed techniques for the detection and quantification of microRNAs, Chem. Soc. Rev. 50 (2021) 4141–4161, https://doi.org/10.1039/d0cs00609b.
[64] M.A. Mori, R.G. Ludwig, R. Garcia-Martin, B.B. Brandao, C.R. Kahn, Extracellular miRNAs: from biomarkers to mediators of physiology and disease, Cell Metabol. 30 (2019) 656–673, https://doi.org/10.1016/j.cmet.2019.07.011.
[65] F. Alhamdan, T. Greulich, C. Daviaud, L.M. Marsh, F. Pedersen, C. Tholken, P. I. Pfefferle, T. Bahmer, D.P. Potaczek, J. Tost, H. Garn, Identification of extracellular vesicle microRNA signatures specifically linked to inflammatory and metabolic mechanisms in obesity-associated low type-2 asthma, Allergy 78 (2023) 2944–2958, https://doi.org/10.1111/all.15824.